KSCE Journal of Civil Engineering (2017) 21(7):2821-2827

DOI 10.1007/s12205-017-0120-1

Structural Engineering

pISSN 1226-7988, eISSN 1976-3808
www.springer.com/12205

TECHNICAL NOTE

Experimental Investigations on VIV of Bridge Deck Sections: A Case Study

Zeng-shun Chen*, Si-meng Liu, Xian-feng Yu***, Cun-ming Ma****, and Lei Liu*****

Received July 8, 2016/Revised November 2, 2016/Accepted December 5, 2016/Published Online February 13, 2017

Abstract

In this paper, the Vortex Induced Vibrations (VIVs) of bridge deck sections of the Hong Kong-Zhuhai-Macao Bridge were investigated experimentally. Aeroelastic tests for the bridge deck of two scale ratios (1:20 model and 1:50 model) under different wind attack angles, wind speeds, and damping ratios were performed. Accessory and windbreak effects on the VIVs of the bridge deck were also carried out. The experimental results show that the accessory and windbreak tend to enlarge the VIVs of the bridge deck. Furthermore, the most unfavorable wind attack angle is 5°. At this attack angle and low damping ratios, the VIVs of the bridge deck are significant and much larger than the allowable value. In addition, the VIVs of the bridge deck decrease with increasing the damping ratios (Particularly, at large damping ratios, the VIVs were well suppressed). This study provides a guideline for the designs of long span flexible bridges on suppressing the VIVs of the bridges.

Keywords: *bridge deck, Vortex Induced Vibrations (VIVs), aeroelastic test, turned mass damper*

1. Introduction

Bridges tend to be long span and flexible, and wind effects on slender bridges are primarily considered during design process. The bridge deck section of long span bridges mainly suffers aeroelastic phenomena of buffeting, VIV as well as flutter or galloping. Buffeting of the bridge deck is characterized random oscillation which is due to wind turbulence (Xu *et al.*, 1998). Flutter and galloping are characterized large oscillations and depend on the motion of the bridge deck. Depending on the deck shape, the VIV of a bridge can occur at low wind speed. A typical wind-bridge interaction appearing in a vortex shedding region may result in large oscillations of the bridge deck. Although the response of VIV is not as dangerous as flutter or galloping, it can influence the fruition and the fatigue life of a bridge deck (Diana *et al*., 2006; Larsen *et al*., 2000; Zhou *et al*., 2015). Therefore, the VIV of the bridge deck and its suppression should be well considered.

Fundamental researches have focused on the VIVs of bluff bodies and a variety of phenomena were obtained (Bearman, 1984; Bearman and OWen, 1998; Ehsan and Scanlan, 1990; Griffin and Hall, 1991; Matsumoto, 1999; Perry *et al*., 1982). The phenomena as well as the mechanism about the VIVs of the bluff bodies with simple configurations were primarily investigated. However, the VIVs of a structure with a more complicated configuration are still suspending to study. For example, a bridge deck section characterized a long afterbody is as a typical bluff body which may exhibit substantially different flow features (Wu and Kareem, 2012). Since the famous dramatic Tacoma Narrows Bridge disaster of 1940 (Billah and Scanlan, 1991), wind-induced vibrations including VIVs of bridges have been widely investigated (Billah, 1989; Ehsan, 1988; Ehsan *et al.*, 1990). Numerous studies have also focused on the VIV suppressions and controls of the bridge decks (Camarri and Iollo, 2010; Du and Sun, 2015; Wu and Kareem, 2013; Zhou *et al*., 2015). A Tuned Mass Damper (TMD) method is acknowledged one of the most effective ways to suppress the wind induced vibrations of a bridge deck and is therefore widely utilized (Fujino and Yoshida, 2002; Morga and Marano, 2014; Xing *et al*., 2013). In the TMD control, the mass block of TMD will move towards opposite direction of the main structure, so the vibration of the main structure can be mitigated. It has been

*Ph.D. Candidate, Engineering Research Center of Bridge Structure and Material in the Mountainous Area (Chongqing Jiaotong University), Ministry of Education, Chongqing, China; Dept. of Civil and Environmental Engineering, The Hong Kong University of Science and Technology, Clear Water Bay, Kowloon, Hong Kong (E-mail: zchenba@ust.hk)

**Associate Professor, Engineering Research Center of Bridge Structure and Material in the Mountainous Area (Chongqing Jiaotong University), Ministry of Education, Chongqing, China (E-mail: simengliu@163.com)

***Associate Professor, State Key Laboratory of Subtropical Building Science, South China University of Technology, Guangzhou, China (E-mail: ctxfyu@scut.edu.cn)

****Associate Professor, School of Civil Engineering, Southwest Jiaotong University, Chengdu, China (Corresponding Author, E-mail: macunming2006@gmail.com)

*****Senior Engineer, Engineering Research Center of Bridge Structure and Material in the Mountainous Area (Chongqing Jiaotong University), Ministry of Education, Chongqing, China (E-mail: liuleill@vip.sina.com)

proved that the control efficiency of a TMD system is sensitive to frequency characteristics and the vibration frequency tends to be affected by many uncertainties (Gu *et al.*, 2001), i.e. vehicle load, flutter deviations. The selection of the controlled mode may also have significant effect on the efficiency. Details can refer to previous studies (Kareem and Kline, 1995; Xing *et al*., 2013). It can reduce the vibration of a system significantly with increasing the damping ratios of the TMD system. It should be noted that the use of a TMD system to suppress the VIV of a bridge deck is possible when the bridge span is short (i.e. hundreds of meters). In this case, only one or two modes of vibration are excited. In case of longer spans, many frequencies can be excited by VIV and the TMD system is not a solution. In this case, aerodynamic measures should be chosen to suppress the VIV of a bridge deck (Brancaleoni and Diana, 1993; Larsen, 1993).

In this study, the HongKong-Zhuhai-Macao Bridge: Jianghai Channel Bridge, whose bridge deck is characterized long afterbody, was taken as a case study to investigate VIVs of the bridge deck. Two wind tunnel experiments (1:20 model and 1:50 model) of the bridge deck under different wind attack angles, wind speeds and damping ratios during the construction and completion stages were conducted. Meaningful results of the VIVs of the bridge deck are obtained and discussed. This study provides a guideline for designs of the long span bridge as well as a Turned Mass Damper (TMD) system on suppressing the VIVs of the bridge deck.

2. Experimental Setup

2.1 Description of the Bridge

The Jianghai Channel Bridge is an across-sea cable-stayed bridge and an important component of the HongKong-Zhuhai-Macao Bridge. It is located at the tropical monsoon climate region of the South Asia, where is frequently affected by the disastrous weather and strong wind. The overall length of the bridge is 994 m and the span arrangement is (110+129+258+258+129+110) m. The bridge girder is a steel box section with a width of 38.8 m and a height of 4.5 m, as shown in Fig. 1(b). The bridge tower is designed as 'Dolphin' exterior and constructed with steel. Its height is 113.756 m. The details of this bridge are presented in Fig. 1.

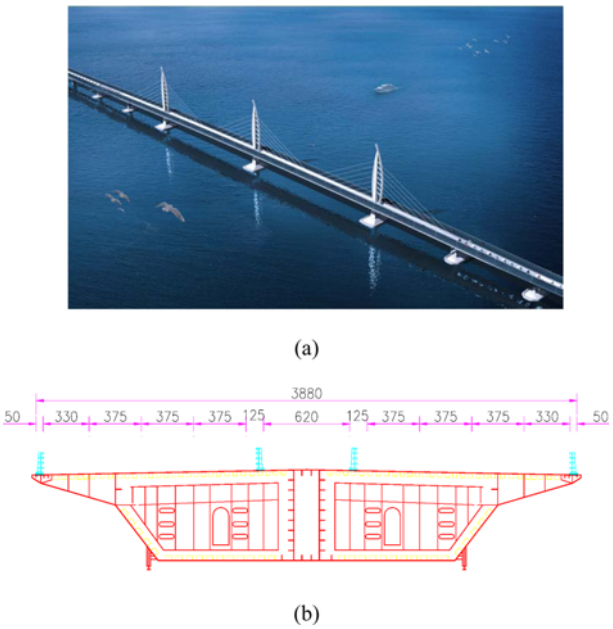

Fig. 1. The Jianghai Channel Bridge: (a) Overview, (b) Dimensions of the Bridge Deck

2.2 VIV Aeroelastic Tests

It should be clarified that the two wind tunnel VIV aeroelastic tests were performed. The difference between the two tests is the scale ratio between the prototype and the test models. The first wind tunnel test was carried out using 1:20 models, and it was found that the VIV occurred and exceeded a calculated allowable value. To decrease the Reynolds number effect and get more accurate results at the VIV range, the second wind tunnel test was performed using 1:50 models (a larger scale ratio). In each test, the two models were tested: one is used for simulating the wind effect on the bridge deck which is in construction stage (without accessories, i.e. guard rail, mat stone, overhaul track, etc., being installed) and the other is used for simulating that in completion stage (with the accessories being installed).

The first Small Scale Wind Tunnel Test (SSWTT) was performed at the second test section of the XNJD-1 wind tunnel (the high wind speed section) of the Southwest Jiaotong University. The test section is 2.4m (width) × 2.0 m (height). The maximum wind speed is 45 m/s and the minimum is 0.5 m/s. The wind profile is determined from the on-site measured parameters and it is directly given as $U_Z/U_{10} = (Z/10)^{0.098}$. The dimensions of the test models (with and without the accessories) are both 2.095 m (length) × 0.776 m (width) × 0.09 m (height). The scale ratio between the prototype and the test model is 1:50. The second wind tunnel test was performed at the XNJD-3 wind tunnel (the low wind speed section) of the Southwest Jiaotong University. The test section is 36 m (length) × 22.5 m (width) × 3.6 m (height). The maximum wind speed is 16.5 m/s and the minimum is 1.0 m/s. The wind profile is the same to that in the first wind tunnel test. The dimensions of the test models are both 3.46 m (length) × 1.94 m (width) × 0.225 m (height). The scale ratio between the prototype and the test model of the bridge sections are 1:20. Other parameters of the test models are presented in Table 1.

The models are suspended on support frames by 8 springs and can oscillate in vertical and torsional directions, as shown in Fig. 2(a). The frequencies and masses of the test models are set through adjusting springs and adding mass blocks at two ends of the models. During the tests, the wind speed is set at an increment of 0.1 m/s at vortex shedding ranges and 0.2 m/s at other ranges. The wind attack angles, as shown in Fig. 2(b), are fixed at α = -5, α = -3, α = 0°, α = 3° and α = 5°. The responses of the test models are measured using laser displacement sensors.

Table 1. Parameters of the Test Models

Parameters		Prototype	1:50 models (First test)	1:20 models (Second test)
Dimension	Length (m)	69.2	2.095	3.46
	Width (m)	38.8	0.776	1.94
	Height (m)	4.5	0.09	0.225
Mass	Construction stage(kg/m)	35580	10.17	83.95
	Completion stage (kg/m)	26780	14.23	66.95
Damping ratio	Construction stage (%)	0.32	0.32	0.32
	Completion stage (%)	0.32	0.32	0.32
Vertical bending frequency	Construction stage (HZ)	0.2536	3.03	3.025
	Completion stage (HZ)	0.3316	2.8	2.88
Torsional frequency	Construction stage (HZ)	1.4039	6.51	/
	Completion stage (HZ)	1.0782	5.95	/

(a)

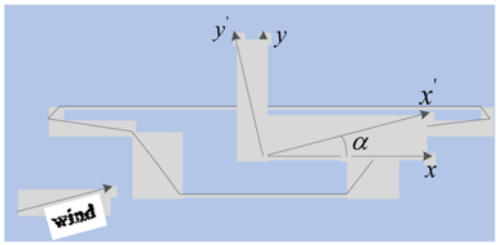

(b)

Fig. 2. Test Models in the Wind Tunnel: (a) Test Model in Wind Tunnel, (b) Wind Attack Angle

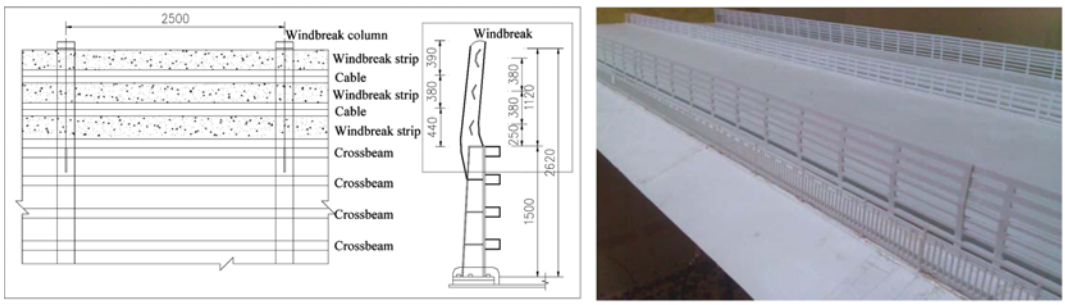

(a) (b)

Fig. 3. The Windbreak of the Bridge: (a) the Details of the Windbreak, (b) Overview of the Windbreak

In order to investigate damping ratio effects on the VIV of the bridge sections, the damping ratios ξ are adjusted from 0.25%-1.35%.

To improve driving environment, windbreaks are considered to be installed after completion of the bridge. However, the windbreaks can have great effect on wind flow (Heisler and Dewalle, 1988; Wilson, 1985) and may have unfavorable effect on the VIV of the bridge deck. Therefore, a wind tunnel test of

the bridge deck with windbreaks being installed was also carried out. The details of the windbreaks are presented in Fig. 3. Other parameters are the same with those in the first wind tunnel test.

3. Experimental Results and Discussions

It should be noted that the allowable value is determined from the Wind-Resistant Design Specification for Highway Bridges (Xiang *et al*., 2004). The allowable amplitudes of the bridge decks in vertical (first-order bending mode) and torsional directions in completion stage are

$$[h_a] = 0.04 / f_h = 0.04 / 0.3316 = 0.1206\text{m}$$

$$[\theta_a] = 4.56 / f_\alpha B = 4.56 / (1.0782 \times 38.8) = 0.109\ rad$$

The allowable amplitudes of the bridge decks in the vertical (first-order bending mode) and torsional directions in construction stage are

$$[h_a] = 0.04 / f_h = 0.04 / 0.2536 = 0.1577\ \text{m}$$

$$[\theta_a] = 4.56 / f_\alpha B = 4.56 / (1.4039 \times 38.8) = 0.084\ rad$$

From the wind tunnel tests, the VIVs of the bridge deck at small damping ratio (0.3%) under different wind attack angles during construction stage are much smaller than the allowable value (see Appendix in Fig. 9) while the VIVs are significant over the same cases in completion stage (Fig. 5). This suggests that accessories have great effect on the VIVs of the bridge decks and tend to enlarge this effect. Furthermore, the VIVs of the bridge deck in completion stage are more prone to occur other than those in construction stage. Therefore, this study focuses on the VIVs of bridge deck in the completion stage (The following results are about the VIVs of bridge deck in completion stage).

3.1 The VIVs of the Bridge Deck from the 1:50 Model

The vertical responses of the bridge decks at a small damping ratio (0.3%) under different wind attack angles and wind speeds (have been transferred in real bridge) are obtained from the 1:50 model, as shown in Fig. 4. It should be noted that the wind speeds in the following figures refer to those acted on the prototype instead of the test model.

In Fig. 4, the wind speeds of the bridge deck vary 5 to 35 m/s, which correspond to reduced wind speeds varying from 3.35 to 23.5 ($U = v/f_hD$). Here, v is the wind speed of the bridge deck (the prototype of the test model); U is the reduced wind speed; f_h is the fundamental frequency of the bridge deck in vertical direction, which is equal to 0.3316 HZ (Table 1); D is the height of the bridge deck, which is equal to 4.5 m (Table 1). In Fig. 4, at a low damping ratio (0.3%), vertical VIVs of the bridge deck occur when the wind attack angles are 3° and 5°. The first peaks around the wind speed of 14 m/s (U = 9.4) are Karman vortex type, which can be explained as a lock-in phenomenon. Therefore, this type of vibration occurs at the reduced wind velocity of 1/*St* (*St* is the Strouhal number). The second peaks around the wind speed range of 25-26 m/s (U =16.8 to 17.4) belongs to the motion-induced vortex type, which is generated by motion-induced vortices due to the shear layer instability (Matsumoto *et al*., 1993; Matsumoto *et al*., 2008). Furthermore, the VIVs of the bridge deck at the wind attack angles of 3° and 5° are much larger than those of the other wind attack angles and exceed the allowable value. The most unfavourable one occurs at the wind attack angle of 5° and the corresponding wind speed is around 26 m/s.

The torsional responses of the bridge deck at a small damping ratio (0.3%) under different wind attack angles and wind speeds (have been transferred in real bridge) are obtained from the 1:20 model, as shown in Fig. 5.

In Fig. 5, the wind speeds of the bridge deck vary 35 to 65 m/s, which correspond to reduced wind speeds varying from 7.2 to 13.4 ($U = v/f_\alpha D$). Here, f_α is the fundamental frequency of the bridge deck in torsional direction, which is equal to 1.0782 HZ. In Fig. 5, the trend of the torsional VIVs is in close agreement with that of the vertical VIVs. Torsional VIVs of the bridge deck also occur when the wind attack angles are 3° and 5°. The VIVs of the bridge deck at the wind attack angles of 3° and 5° are much larger than those of other wind attack angles and exceed the

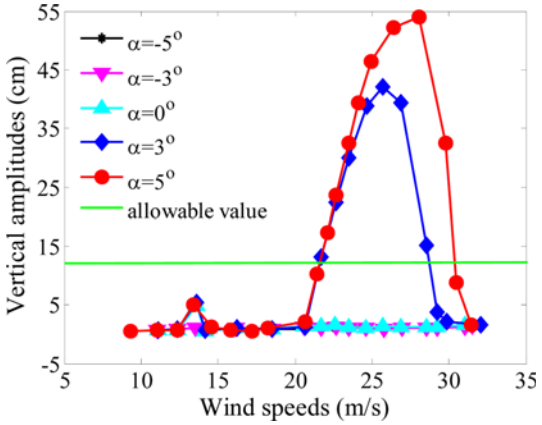

Fig. 4. The Vertical Responses Under Different Wind Attack Angles (Damping Ratio = 0.3%)

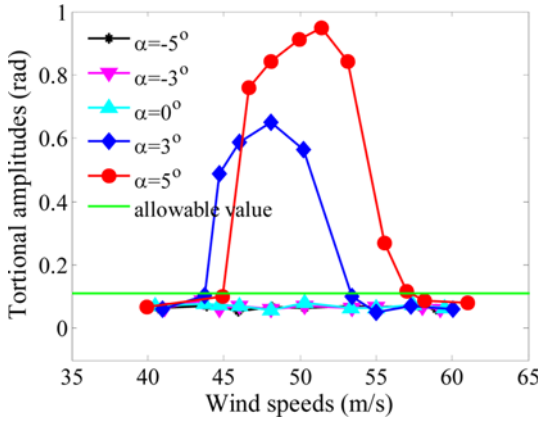

Fig. 5. Torsional Responses Under Different Wind Attack Angles (damping ratio=0.3%)

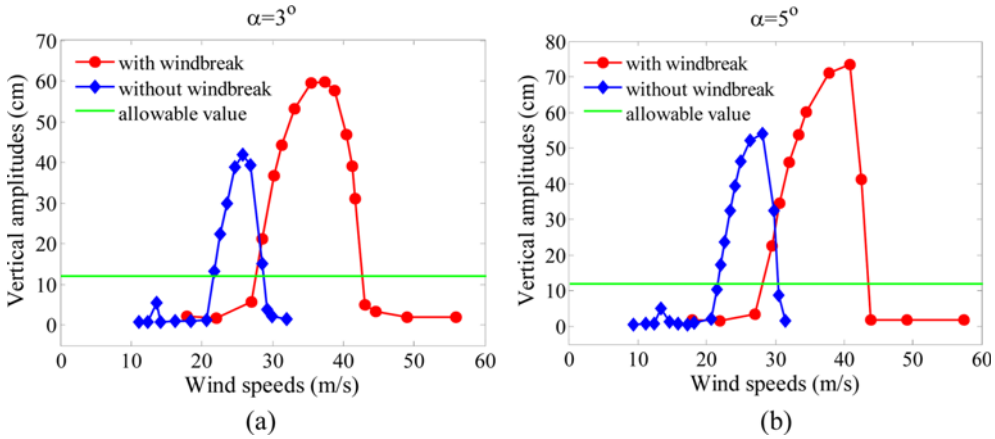

Fig. 6. Windbreak Effect on VIVs of the Bridge Deck (Damping Ratio = 0.3%): (a) Wind Attack Angle 3°, (b) Wind Attack Angle 5°

allowable value. The most unfavourable one occurs at the wind attack angle of 5° and the corresponding wind speed is around 51 m/s which rarely happens at the bridge site.

As mentioned, windbreaks are considered to be installed after completion of the bridge to improve driving environment. However, this may enlarge VIVs of the bridge deck. Windbreak effect on the VIVs of the bridge deck should be acquired. The VIVs of the bridge deck under different wind speeds with and without windbreak cases are presented in Fig. 6.

In Fig. 6, the vertical amplitudes in the wind attack angle of 5° case are larger than those in 3° case. In each case, the VIVs of the bridge deck with windbreaks are larger than those without windbreaks and they are all much larger than the allowable value. This suggests that windbreaks can enlarge the VIVs of the bridge deck and have unfavorable effect on it. This trend is in close agreement with that of aforementioned accessory effect (Accessory would enlarge the VIVs of the bridge deck). The possible reason is that the windbreaks abrupt the flow separation and reattachment from the windbreaks and from the leading edge corners of the bridge. The distributed porosity and height of the windbreaks may also have significant effect on VIVs of a bridge deck. The effect is complicated and it is usually investigated from flow filed (i.e. PIV and CFD).

From above illustrations, vertical and torsional VIVs exceed to the allowable value at wind attack angles of 3° and 5°. The torsional VIV wind speeds are much larger than the vertical ones. This suggests the vertical VIVs of the bridge deck are more prone to occur than the torsional VIVs. Furthermore, the most unfavorable wind attack angle is 5° in the vertical VIVs of the bridge deck. In addition, the above results are obtained from a small scale ratio model (1:50) and the Reynolds number and geometry may have significant effect on the precision of the results. To reduce this effect, a larger scale ratio model (1:20) is selected.

3.2 VIVs of the Bridge Deck from the 1:20 Model

As mentioned before, the the vertical VIVs of the bridge deck are much more prone to occur than the torsional VIVs and the torsional VIVs occur only at very large wind speed which rarely happen at the site of the bridge. Thus, in this section, only vertical VIV and its suppression of the bridge deck are concerned. Vertical responses of the bridge decks at a small damping ratio (0.25%) under different wind attack angles and wind speeds (have been transferred in real bridge) are obtained from the 1:20 model, as shown in Fig. 7.

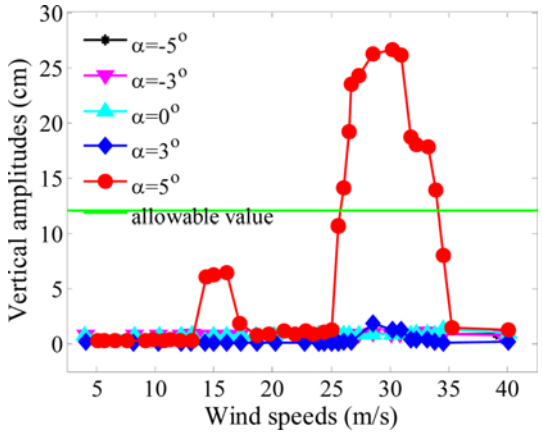

Fig. 7. Vertical Responses Under Different Wind Attack Angles (damping ratio = 0.25%)

In Fig. 7, the corresponding reduced wind speeds vary from 3.35 to 26.8 (5 m/s to 40 m/s). The first peak occurs at the wind speed of 15.5 m/s ($U = 10.39$), which is ascribed to lock-in phenomenon and close to the reduced wind speed of $1/St$. Furthermore, the significant VIVs of the bridge deck occur only at a wind attack angle of 5° and the amplitudes and corresponding wind speeds are slightly different from those obtained from the small scale ratio model (1:50 one). The differences may be ascribed to different flow patterns around the models (i.e. different flow separation and reattachment). Furthermore, they may also be affected by the different local Reynolds number. Besides, the differences may also be induced by measurement errors. From Fig. 7, the most unfavorable VIVs of the bridge deck occur at the wind attack angle of 5°, which is much larger

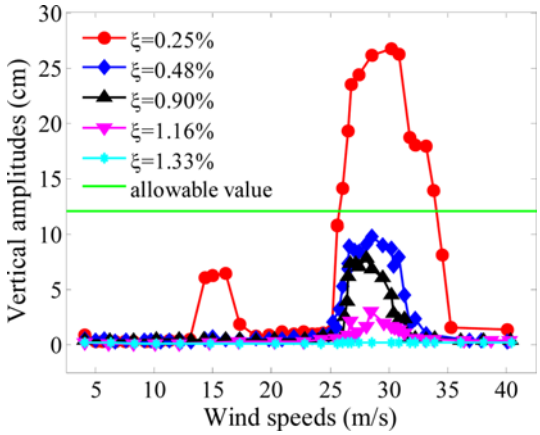

Fig. 8. Vertical Responses Under Different Damping Ratios (wind attack angle = 5°)

than the allowable value. This should be well concerned and solved. As mentioned, for short-span bridges, TMD is an effective way to solve this problem and generally used to suppress the wind induced vibrations of slender structures including bridge decks (Abdel-Rohman and Askar, 1996; Morga and Marano, 2014). It is realized through a device mounted in structures to add the mass and damper of the structures. The basic principal is to add damper of the structures to reduce the amplitude of mechanical vibrations. Based on this, the most unfavorable wind attack angle 5° is selected and damping ratios are varied to study their effects on VIVs of the bridge deck, as shown in Fig. 8.

From Fig. 8, at very low damping ratios (e.g. 0.25%), the maximum vertical VIV of the bridge deck is 26.65 cm which is much larger than the allowable value (around 12 cm). When the damping ratio is increased to 0.48%, the maximum vertical VIV of the bridge deck is significantly decreased to 9.79 cm which is lower than the allowable value. It is found that the VIVs of the bridge deck tend to decrease with increasing the damping ratios. Specifically, at large damping ratios, the VIVs of the bridge deck are well suppressed and are much lower than the allowable value. For example, the maximum vertical VIV is 3.08 cm when the damping ratio is 1.16% and the VIV does not occur when the damping ratio is increased to 1.33%. This suggests that the VIVs of the bridge deck can be well suppressed through improving the damping ratio of the bridge.

From the above discussions, for the bridge deck in construction stage, VIVs of the bridge deck are weak and much lower than the allowable value under five wind attack investigated here angles and any damping ratios. The accessories and windbreaks have unfavorable effect to VIVs of the bridge deck and can increase the VIVs of it. For the bridge deck in completion stage, the most unfavourable wind attack angle is 5°. At this wind attack angle, VIVs of the bridge deck are significant under low damping ratios (e.g. lower than 0.25%) and are much large than the allowable value. Furthermore, improving damping ratios of the bridge is an effective way to suppress the VIVs of the bridge deck. This provides a guideline for designing a TMD system for suppressing the VIVs of the bridge.

4. Conclusions

The VIVs of long afterbody bridge decks tend to occur and should be well concerned. In this study, the VIVs of the bridge decks of the HongKong-Zhuhai-Macao Bridge: Jianghai Channel Bridge under different wind attack angles, damping ratios and wind speeds were studied experimentally. Meaningful results of the VIVs of the bridge were summarized as follows:

1. The VIVs of the bridge decks in construction stage (without accessories being installed) are weak and much smaller than the allowable value. The VIVs of bridge decks with the windbreaks are larger than those without windbreaks. This suggests that accessories and windbreaks of bridge decks are unfavorable to the VIVs and tend to enlarge the VIVs of the bridge decks.
2. The most unfavorable wind attack angle is 5°. The VIVs of the bridge deck are significant and the maximum ones are much larger than the allowable values at this wind attack angle and low damping ratios.
3. Damping ratios have great effect on the VIVs of the bridge deck. The VIVs of the bridge deck tend to decrease with increasing the damping ratios and the VIVs are weak or do not occur at large damping ratios. This suggests the VIVs of the bridge deck can be well suppressed through improving the damping ratio of the bridge.

Acknowledgements

This work described in this paper is partially supported by the Engineering Research Center of Bridge Structure and Material in the Mountainous Area (Chongqing Jiaotong University), Ministry of Education of China (QLGCZX-JJ2015-6,QLGCZX-JJ2015-5); The State Key Laboratory Breeding Base of Mountain Bridge and Tunnel Engineering (Chongqing Jiaotong University) fund (CQSLBF-Y16-16); The Natural Science Foundation of China under the Grants (No.: 51408087 and No.:51278435) and the "Xiaoping Science and Technology Innovation Team" fund for Chinese college students.

References

Abdel-Rohman, M. and Askar, H. (1996). "Control by passive TMD of wind-induced nonlinear vibrations in cable stayed bridges." *Journal of Vibration and Control,* Vol. 2, No. 2, pp. 251-267, DOI: 10.1177/107754639600200206.

Bearman, P. W. (1984). "Vortex shedding from oscillating bluff bodies." *Annual Review of Fluid Mechanics,* Vol. 16, No. 1, pp. 195-222, DOI: 10.1146/annurev.fl.16.010184.001211.

Bearman, P. W. and OWen, J. C. (1998). "Reduction of bluff-body drag and suppression of vortex shedding by the introduction of wavy separation lines." *Journal of Fluids and Structures*, Vol. 12, No. 1, pp. 123-130, DOI:10.1006/jfls.1997.0128.

Billah, K. Y. and Scanlan, R. H. (1991). "Resonance, Tacoma Narrows bridge failure, and undergraduate physics textbooks." *American Journal of Physics*, Vol. 59, No. 2, pp. 118-124, DOI: 10.1119/1.16590.

Billah, K. Y. R. (1989). *A study of vortex-induced vibration*, Doctoral

Dissertation, Princeton University.
Brancaleoni, F. and Diana, G. (1993). "The aerodynamic design of the Messina Straits Bridge." *Journal of Wind Engineering and Industrial Aerodynamics,* Vol. 48, Nos. 2-3, pp. 395-409, DOI: 10.1016/0167-6105(93)90148-H.
Camarri, S. and Iollo, A. (2010). "Feedback control of the vortex-shedding instability based on sensitivity analysis." *Physics of Fluids (1994-present)*, Vol. 22, No. 9, 094102, DOI: 10.1063/1.3481148.
Diana, G., Resta, F., Belloli, M., and Rocchi, D. (2006). "On the vortex shedding forcing on suspension bridge deck." *Journal of Wind Engineering and Industrial Aerodynamics*, Vol. 94, No. 5, pp. 341-363, DOI: 10.1016/j.jweia.2006.01.017.
Du, L. and Sun, X. (2015). "Suppression of vortex-induced vibration using the rotary oscillation of a cylinder." *Physics of Fluids (1994-present)*, Vol. 27, No. 2, 023603, DOI: 10.1063/1.4913353.
Ehsan, F. (1988). *The vortex-induced response of long, suspended-span bridges*, Doctoral Dissertation, Johns Hopkins University.
Ehsan, F. and Scanlan, R. H. (1990). "Vortex-induced vibrations of flexible bridges." *Journal of Engineering Mechanics*, Vol. 116, No. 6, pp. 1392-1411, DOI: 10.1061/(ASCE)0733-9399(1990)116:6(1392).
Ehsan, F., Scanlan, R. H., and Bosch, H. R. (1990). "Modeling spanwise correlation effects in the vortex-induced response of flexible bridges." *Journal of Wind Engineering and Industrial Aerodynamics*, Vol. 36, No. 2, pp. 1105-1114, DOI: 10.1016/0167-6105(90)90107-N.
Fujino, Y. and Yoshida, Y. (2002). "Wind-induced vibration and control of Trans-Tokyo Bay crossing bridge." *Journal of Structural Engineering*, Vol. 128, No. 8, pp. 1012-1025, DOI: 10.1061/(ASCE)0733-9445(2002)128:8(1012), 1012-1025.
Griffin, O. M. and Hall, M. (1991). "Review—vortex shedding lock-on and flow control in bluff body wakes." *Journal of Fluids Engineering*, Vol. 113, No. 4, pp. 526-537, DOI: 10.1115/1.2926511.
Gu, M., Chen, S., and Chang, C. (2001). "Parametric study on multiple tuned mass dampers for buffeting control of Yangpu Bridge." *Journal of Wind Engineering and Industrial Aerodynamics*, Vol. 89, No. 11, pp. 987-1000, DOI: 10.1016/S0167-6105(01)00094-0.
Heisler, G. M. and Dewalle, D. R. (1988). "2. Effects of windbreak structure on wind flow." *Agriculture, Ecosystems & Environment,* Vol. 22, pp. 41-69, DOI: 10.1016/0167-8809(88)90007-2.
Kareem, A. and Kline, S. (1995). "Performance of multiple mass dampers under random loading." *Journal of Structural Engineering*, Vol. 121, No. 2, pp. 348-361, DOI: 10.1061/(ASCE)0733-9445(1995)121:2(348), 348-361.
Larsen, A. (1993). "Aerodynamic aspects of the final design of the 1624 m suspension bridge across the Great Belt." *Journal of Wind Engineering and Industrial Aerodynamics*, Vol. 48, Nos. 2-3, pp. 261-285, DOI: 10.1016/0167-6105(93)90141-A.
Larsen, A., Esdahl, S., Andersen, J. E., and Vejrum, T. (2000). "Storebælt suspension bridge–vortex shedding excitation and mitigation by guide vanes." *Journal of Wind Engineering and Industrial Aerodynamics*, Vol. 88, No. 2, pp. 283-296, DOI: 10.1016/S0167-6105(00)00054-4.
Matsumoto, M. (1999). "Vortex shedding of bluff bodies: A review." *Journal of Fluids and Structures*, Vol. 13, Nos. 7-8, pp. 791-811, DOI: 10.1006/jfls.1999.0249.
Matsumoto, M., Shiraishi, N., Shirato, H., Stoyanoff, S., and Yagi, T. (1993). "Mechanism of, and turbulence effect on vortex-induced oscillations for bridge box girders." *Journal of Wind Engineering and Industrial Aerodynamics,* Vol. 49, Nos. 1-3, pp. 467-476, DOI: 10.1016/0167-6105(93)90041-L.
Matsumoto, M., Yagi, T., Tamaki, H., and Tsubota, T. (2008). "Vortex-induced vibration and its effect on torsional flutter instability in the case of B/D = 4 rectangular cylinder." *Journal of Wind Engineering and Industrial Aerodynamics,* Vol. 96, No. 6, pp. 971-983, DOI: 10.1016/j.jweia.2007.06.023.
Morga, M. and Marano, G. C. (2014). "Optimization criteria of TMD to reduce vibrations generated by the wind in a slender structure." *Journal of Vibration and Control,* Vol. 20, No. 16, pp. 2404-2416, DOI: 10.1177/1077546313478296.
Perry, A., Chong, M., and Lim, T. (1982). "The vortex-shedding process behind two-dimensional bluff bodies." *Journal of Fluid Mechanics*, Vol. 116, pp. 77-90, DOI: 10.1017/S0022112082000378.
Wilson, J. D. (1985). "Numerical studies of flow through a windbreak." *Journal of Wind Engineering and Industrial Aerodynamics,* Vol. 21, No. 2, pp. 119-154, DOI: 10.1016/0167-6105(85)90001-7.
Wu, T. and Kareem, A. (2012). "An overview of Vortex-induced Vibration (VIV) of bridge decks." *Frontiers of Structural and Civil Engineering,* Vol. 6, No. 4, pp. 335-347, DOI: 10.1007/s11709-012-0179-1.
Wu, T. and Kareem, A. (2013). "Vortex-induced vibration of bridge decks: Volterra series-based model." *Journal of Engineering Mechanics*, Vol. 139, No. 12, pp. 1831-1843, DOI: 10.1061/(ASCE)EM.1943-7889.0000628, 1831-1843.
Xiang, H., Bao, W., Chen, A., Lin, Z., and Liu, J. (2004). *Wind-resistant design specification for highway bridges*, Ministry of Communications of the People's Republic of China (In Chinese).
Xing, C., Wang, H., Li, A., and Xu, Y. (2013). "Study on wind-induced vibration control of a long-span cable-stayed bridge using TMD-type counterweight." *Journal of Bridge Engineering*, Vol. 19, No. 1, pp. 141-148, DOI: 10.1061/(ASCE)BE.1943-5592.0000500, 141-148.
Xu, Y., Sun, D., Ko, J., and Lin, J. (1998). "Buffeting analysis of long span bridges: A new algorithm." *Computers & Structures*, Vol. 68, No. 4, pp. 303-313, DOI: 10.1016/S0045-7949(98)00072-8.
Zhou, Z., Yang, T., Ding, Q., and Ge, Y. (2015). "Mechanism on suppression in vortex-induced vibration of bridge deck with long projecting slab with countermeasures." *Wind Struct*, Vol. 20, No. 5, pp. 643-660, DOI: 10.12989/was.2015.20.5.643.

Appendix

It should be clarified that Fig. 9 presented here is used for comparison. From Fig. 9, VIVs of the bridge decks at small damping ratio (0.3%) under different wind attack angles during construction stage (without accessories being installed) are weak or do not occur and much smaller than the allowable value.

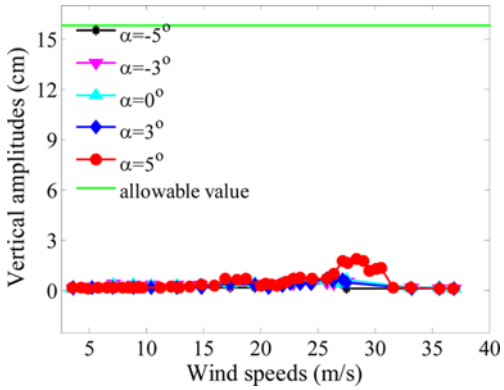

Fig. 9. Vertical Amplitudes for the Construction Stage Model (without accessories being installed, damping ratio=0.3%) Under Different Wind Attack Angles and Wind Speeds